

# Resistive layers formation during the superconductor-normal transition of high- $T_c$ superconductors

Linda Ponta\*, Anna Carbone\*, Marco Gilli† and Piero Mazzetti\*

\*Physics Department, Politecnico di Torino,

Corso Duca degli Abruzzi 24, 10129 Torino, Italy

Email: linda.ponta@polito.it, anna.carbone@polito.it, piero.mazzetti@polito.it

†Electronic Engineering Department, Politecnico di Torino,

Corso Duca degli Abruzzi 24, 10129 Torino, Italy

Email: marco.gilli@polito.it

**Abstract**—The formation of layers during the resistive transition of granular high- $T_c$  superconductors, characterized by either weak (YBCO-like) or strong ( $MgB_2$ -like) links, occurs through a series of avalanche-type current density rearrangements. These resistive layers cross the whole specimen approximately orthogonal to the current density direction, and are due to the simultaneous transition of a large number of weak-links or grains. In the present work, strongly and weakly linked networks of nonlinear resistors, with Josephson junction characteristics are considered. It is shown that the exact solution of the Kirchhoff equations yields the subsequent formation of resistive layers within the superconductive matrix as temperature increases. Furthermore, the resistive layer formation process is related to the voltage noise observed at the transition. At the end of the transition, as experimentally found, the layers mix-up, the step amplitude decreases and the resistance curve smoothes. The approach can be extended to networks with arbitrary size and, thus, to real specimens.

## I. INTRODUCTION

Depending on physical conditions, material type and structure, diverse mechanisms can regulate the superconductive-normal state transition. In type II superconductors at  $T \ll T_c$ , where  $T_c$  is the critical temperature in the absence of magnetic field and current, the transition occurs when fluxoids, injected by external magnetic fields or strong bias current densities, begin to move causing energy losses and heating. This is relevant for the development of high-field superconducting magnets [1]–[10]. When temperature is close to  $T_c$  at low current density, a different transition mechanism may occur. In this case, an intermediate state may be obtained, characterized by a mixture of superconductive and normal domains. This situation was first studied by Landau and Ginzburg in metals [11], [12]. Recently, it has been considered to explain the excess noise in metallic or high- $T_c$  superconductors transition edge sensors (TES) used as bolometers to detect electromagnetic radiation at the level of single photons [13]–[15].

The excess noise observed during a transition sheds light on the microscopic processes underlying the transition itself [16]–[20]. In [19], the noise observed during the superconductor-normal transition in granular  $MgB_2$  films has been ascribed

to the subsequent formation of resistive layers, with grains in the normal or in the intermediate state, between equipotential superconducting domains. The excess noise derives from the fact that each elementary event -the formation of a layer- implies the simultaneous resistive transition of several grains and, thus, gives rise to a voltage pulse of rather high amplitude (*avalanche noise*).

The present work is addressed to simulate the transition events occurring at granular level responsible for the avalanche-type noise in YBCO-like and  $MgB_2$ -like superconductors [19], [21]. The superconducting material is modeled as a network of Josephson junctions with Gaussian distribution of critical currents. The Josephson junctions represent either weak links between grains (YBCO-like) or grains with strong links ( $MgB_2$ -like). In the strong link case, couples or triples of resistors are used to represent two or three current components flowing through each grain respectively for two-(2D) and three-dimensional (3D) networks. The solutions of Kirchhoff equations for these networks are found by an iterative routine described in the next section. The main results of this analysis are that the resistive transition undergoes discrete step-like increments both in weak and strong link materials. The steps correspond to the creation of resistive layers constituted by grains or weak links in the normal or in the intermediate state. As temperature increases, grains or weak-links in the intermediate state gradually switch to the normal state. The trailing edge of the resistive transition grows more smoothly in  $MgB_2$ -like than in YBCO-like networks. This fact is related to the higher correlation when the elementary transition events occur in triplets rather than in independent nonlinear resistors. At the end of the transition, the resistive layers mix up. The resistance steps become smaller and the transition curve smoother.

## II. MODEL

Among the main physical parameters relevant to the electronic behavior of granular superconductors [22], [23], it is worthy to remind the phase transition boundary of granular

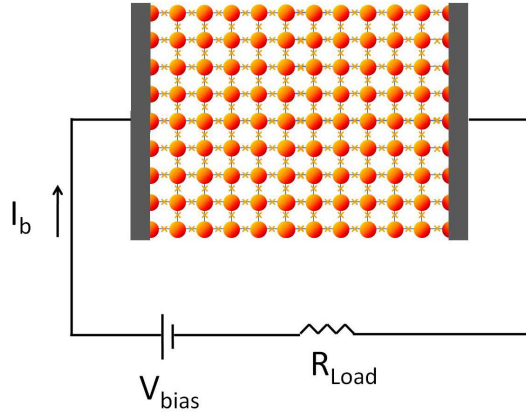


Fig. 1. 2D network scheme of a granular superconductor. The network contains 90 grains. In case of granular superconductors with weak-links (YBCO-like), the grains are assumed to remain in the superconducting state during the transition. Each link between grains is a nonlinear resistor with the  $I - V$  characteristic represented in Fig. 2a. In case of granular superconductors with strong-links ( $\text{MgB}_2$ -like), the  $I - V$  characteristic given in Fig. 2 concerns the whole grain. The first and last node correspond to the electrodes.

superconductors. It is set by the value of the dimensionless tunneling conductance  $g = G/(e^2/\hbar)$ , where  $G$  is the average tunneling conductance between adjacent grains and  $e^2/\hbar$  the quantum conductance. Samples with the normal state conductance greater than the quantum conductance (i.e. with the  $g \gg 1$ ) become superconducting at low temperature [24], regardless of the ratio of Josephson  $J = \pi/2g\Delta$  (with  $\Delta$  the superconductor gap) and Coulomb  $E_c = e^2/C_j$  energies (with  $C_j$  the grain capacitance). This behavior is supported by the experiments.

This phenomenon can be accounted by the electron tunneling between grains, in addition to the Josephson coupling [25]. The additional dissipative tunneling channel results in a reduction of the Coulomb energy to the value  $\tilde{E}_c = \Delta/(2g)$ , known as the effective Coulomb energy of the grain. For  $g \gg 1$ ,  $J$  is always larger than  $\tilde{E}_c$ , implying a superconducting ground state, regardless of the Coulomb energy  $E_c$ . For  $g \gg 1$ , the granular superconductor can then be modeled within the mean-field BCS theory. Thus, its critical temperature is approximately given by the single grain BCS critical temperature  $2\Delta = 3.53kT_c$ . Conversely, for  $g \ll 1$ , the phase transition boundary between insulating and superconducting states is controlled by the ratio between  $J$  and  $E_c$ . In this condition, by using a mean field approach, the critical temperature is given by  $T_c = (1/4)z\pi g\Delta$ , with  $z$  the coordination number of the lattice [22], [23].

The superconductor-normal transition in thin granular films with  $g \gg 1$  can be modeled in terms of resistively shunted Josephson junctions, whose state is controlled only by the value of the normal resistance, rather than by the Coulomb and Josephson energies. The simulations presented in this work have been performed in the regime  $g \gg 1$ , to guarantee the onset of a superconductivity state at low temperature.

In order to simulate the superconductor-normal transition in

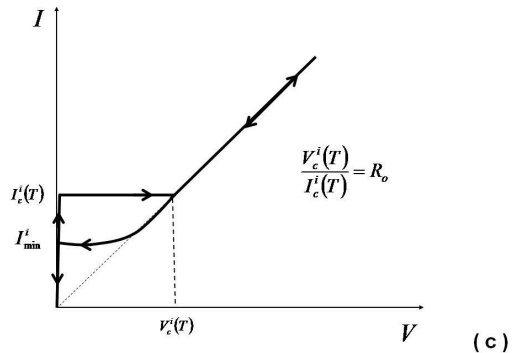
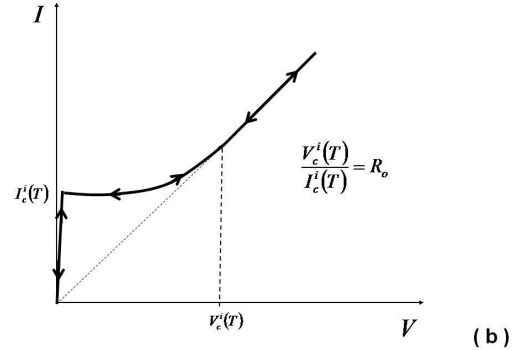
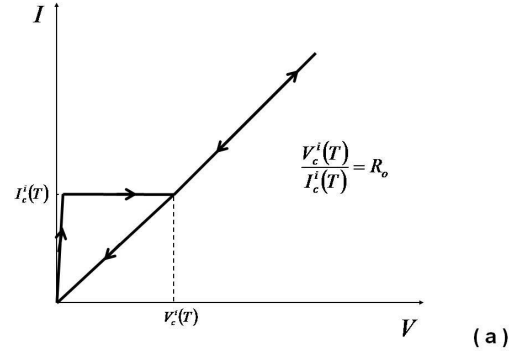


Fig. 2. Josephson junction  $I - V$  characteristics for grains or weak-links in case of underdamped (a), overdamped (b), generalized (c).  $I_{min}^i$  depends on the Stewart-McCumber parameter  $\beta_c$  and ranges from  $I_c^i$  and 0 for  $\beta_c \geq 0$ , where  $\beta_c = \tau_{RC}/\tau_J$ , where  $\tau_{RC}$  and  $\tau_J$  are the capacitance and Josephson time constant respectively.  $\beta_c \gg 1$  in the case (a),  $\beta_c \ll 1$  in the case (b) and  $\beta_c \sim 1$  in the case (c)

granular materials, the network, shown in Fig. 1, is considered. The network is constituted by Josephson junctions, biased by a constant current  $I_b$ . The resistive transition is estimated by solving a system of Kirchhoff equations, at varying temperature.

The network of Fig. 1 can be referred both to YBCO-like materials, characterized by weak-links [26] and to  $\text{MgB}_2$ -like materials [27]–[31], whose transition involves directly the grains. In YBCO-like materials, the transition occurs in two separated steps: first, at lower temperatures, for the weak-links and, then, at higher temperatures, for the grains. The network

of Fig. 1 is used to model the first stage of the transition, which involves only the weak-links, while the grains remain superconductive. In MgB<sub>2</sub>-like, the transition involves also the grains. The current density within the grain sets the state (superconductive, intermediate, normal) of the grain according to its  $I - V$  characteristic. The different behavior of the two type of superconductors is pointed out by introducing the intragrain conductance  $g_{intr}$ . For standard granular system, the condition  $g \ll g_{intr}$  holds.

The intragrain conductance of the weak-link network is much greater than 1 ( $g_{intr} \gg 1$ ). The intragrain region is indeed assumed to remain in the superconducting state, since the transition occurs only at the weak-links. Conversely for the strong-link network the condition  $g \sim g_{intr}$  holds, corresponding to an homogeneously disordered granular system. This condition is consistent with the electronic properties of MgB<sub>2</sub>-like superconductors [27]. The intragrain conductance  $g_{intr}$  is related to the single grain Thouless energy  $E_{Th}$  and to the interlevel spacing  $\delta$  through  $g_{intr} = E_{Th}/\delta$ . When the energy  $E_{Th}$  exceeds the mean level spacing  $\delta$ , it is  $g_{intr} \gg 1$ . The Thouless energy is defined by  $E_{th} = D_o/a^2$ , with  $D_o$  and  $a$  the diffusion coefficient and the radius of the grain. The interlevel spacing is defined  $\delta = 1/(\nu V)$  with  $\nu$  and  $V$  the density of states at the Fermi energy and the volume of the grain. The intragrain conductance strongly depends on the dirtiness of material and the radius of grain. These aspects are indeed relevant for MgB<sub>2</sub>-like materials whose critical temperature is strongly dependent on material quality, atomic radii and cell size [28], [31]. For the sake of simplicity, all the grains are assumed to be isotropic and with the same average size, therefore the anisotropy effects are disregarded [32]–[34]. This assumption is not limitative for what concerns the main aspects of the transition. It allows one to define a critical current  $I_c^i(T)$  characterizing the grain  $i$ , according to a Gaussian distribution, and a normal state resistance  $R_o$  equal for all the grains. In real specimens, small changes of the grain stoichiometry influence the critical current more than the normal state resistivity. The slope of the transition curve depends on the spread of the distribution of the critical currents and temperatures [35]. The normal state resistance  $R_o$  is achieved when the current  $I_i$  crossing the grain or the weak-link exceeds  $I_c^i(T)$ . The intermediate states are characterized by current  $I_c^i(T)$  and voltage drop between 0 and  $V_c^i(T)$ . The  $I - V$  characteristic of each non-linear resistor, representing a grain or a weak-link, is completely defined by the quantities:  $I_c^i(T)$  and  $R_o$ . The quantity  $V_c = I_c^i(T)R$  is directly related to the Josephson time constant  $\tau_J = \Phi_o/(2\pi)$  for the intermediate states ( $0 < v < V_c$ ) and  $\tau_J = \Phi_o/(2\pi I_c R_o)$  for the normal states ( $v > V_c$ ). The characteristic switching time during the transition is defined by these time constants, that are ultimately related to the behavior of noise. In the next section, the simulation of the resistive transition has been performed in networks with (a) underdamped, (b) overdamped and (c) general  $I - V$  characteristics. The I-V curves are characterized by the Stewart-McCumber parameter  $\beta_c = \tau_{RC}/\tau_J$ , where  $\tau_{RC}$  and  $\tau_J$  are the capacitance and Josephson time constant.

$\beta_c \gg 1$  in the case (a),  $\beta_c \ll 1$  in the case (b) and  $\beta_c \sim 1$  in the case (c). In particular, upon cooling the granular system from the normal to the superconductive state the onset of hysteresis has been analyzed.

When the transition involves the grains (strong-links), the current is given by:  $I_i = \left[ \sum_{j=1}^3 I_{ij}^2 \right]^{1/2}$ , where  $I_{ij}$  corresponds to the current flowing from the grain  $i$  to its neighboring grains  $j$  through each resistor of the triplet. The  $I - V$  characteristic is then used to find the value of the three resistors by means of an iterative routine to solve Kirchhoff equations. The grains are assumed isotropic, thus the three resistors representing the grain have identical  $I - V$  characteristics.

The simulations are carried on at constant bias current and the transition is caused by a temperature increase, which reduces the critical currents of the grains or weak-links according to the following linearized equation:

$$I_c^i(T) = I_{co}^i \left( 1 - \frac{T}{T_c} \right) , \quad (1)$$

where  $I_{co}^i$  is the low-temperature critical current, distributed according to a Gaussian function with standard deviation  $\Delta I_{co}$  and mean value  $I_{co}$ .

The preliminary steps of the simulations are the creation of the list of all the  $N_o$  nodes of the network and the introduction of the Gaussian distribution for the critical current  $I_{co}^i$ . Then the iterative calculations are implemented. The vector  $W_o$  of the tentative potential values is defined for all the  $N_o$  nodes. Then, by using the  $I - V$  characteristics, in case of weak-links a conductance value  $G_{ij}$  for each resistor between the nodes  $i$  and  $j$  is calculated. Alternatively, for the strong-link network, the conductance values, common to the three resistors, representing each grain  $i$ , are calculated by using the voltage drop  $V_i = \left[ \sum_{j=1}^3 V_{ij}^2 \right]^{1/2}$ . Once the  $G_{ij}$  are known, the entries of the conductance matrix  $\underline{\underline{G}}$  are:

$$G_{ij} = -G_{ji} \quad (i, j = \text{contiguous}) , \quad (2a)$$

$$G_{ij} = 0 \quad (i, j = \text{not contiguous}) , \quad (2b)$$

$$G_{ii} = \sum_{k \in V_i} G_{ik} , \quad (2c)$$

where  $G_{ik}$  are the conductances of the resistors connected to the node  $i$ .

Then, a new vector of node potentials  $W_1$  is evaluated by solving the equation:

$$\underline{\underline{G}} \cdot W_1 = I_{inj} , \quad (3)$$

with respect to  $W_1$ .  $I_{inj}$  is a vector of dimension  $N_o$ , whose elements are zero except the first one equal to the bias current  $I_b$ . It represents the external current injected into the first electrode. The second electrode is grounded.

Then, the new set of potentials  $W_1$  allows to evaluate a new set of  $G_{ij}$  and a new conductance matrix  $\underline{\underline{G}}$ . From Eq. (3) an updated vector  $W_2$  is then obtained. The iteration is repeated until the quantity  $\varepsilon = |W_n - W_{n-1}|/|W_n|$  becomes smaller than a value  $\varepsilon_{min}$  chosen to exit from the loop. In the present

work, the simulations have been performed by varying  $\varepsilon_{min}$  in the range  $10^{-7} < \varepsilon_{min} < 10^{-11}$  to check that the value of  $\varepsilon_{min}$  did not appreciably change the final solution. The total network resistance  $R$  is then given by  $W_n(1)/I_b$  for each value of  $T/T_c$ , where  $W_n(1)$  is the potential drop at the contact ends. The potential drops at the ends of each resistor for the case of weak links and across the grain for the case of strong links are compared to the values of the potential in the corresponding  $I - V$  characteristics, in order to distinguish weak-links or grains respectively in the superconducting, normal or intermediate state.

### III. SIMULATION RESULTS

The successive stages of the resistive transition are simulated in granular superconducting materials with either strong or weak links. The superconducting material is represented as a network of nonlinear resistors having resistively and capacitively shunted Josephson junction characteristics [36]–[40]. In this section, the results of different simulations, carried on with 2D and 3D networks, both for strong and weak-link transition are reported. In the simulations, the transition occurs by increasing the temperature, in proximity of the critical temperature  $T_c$ , starting from the superconductive state.

Fig. 3 refers to the resistive transition of a three-dimensional  $10 \times 10 \times 10$  network, representing a granular superconducting film of 1000 grains characterized by strong links ( $MgB_2$  type).

Fig. 4 refers to a three-dimensional  $10 \times 10 \times 10$  network, representing a superconducting film of 1000 grains characterized by weak-links (YBCO type).

$R$  and  $T$  are expressed as reduced quantities. The relevant energy values can be found in [20]. The parameters used for the simulations are reported in the figure captions. In Fig. 3, at the beginning of the transition, the network resistance is zero, since all the grains are in the superconductive state. By effect of the temperature increase, a layer of grains either in the normal resistive (green) or in the intermediate (dark blue) state, crossing the whole film, is generated (Fig. 3 (a)). This layer must separate two equipotential superconductive regions and, thus, the potential drop must be constant along the layer. Since the grains have different critical currents, the layer starts to form when the sum of critical currents of its grains equals the bias current. The grain (or the weak-link) with the lowest critical current becomes resistive and set the voltage drop of the other grains in the layer. As temperature increases and critical current decreases, more and more grains in the intermediate state gradually switch to the resistive states and the layer resistance increases.

As shown in Fig. 3 (a), a resistive layer contains at least one resistive (green) dot and many dots in the intermediate state (dark blue). Superconductive (orange) dots are excluded since they would constitute a short. The formation of a resistive layer corresponds to a step in the  $R$  vs  $T$  curve. Upon further temperature increase, other layers are created until the whole film undergoes the transition to the normal state.

At the beginning of the transition the layers are well

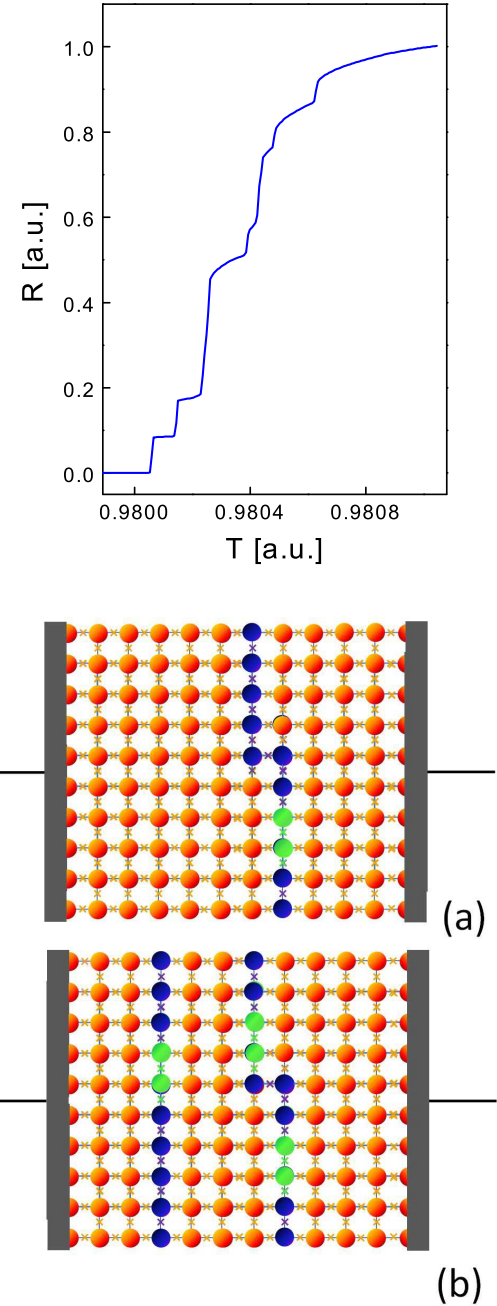


Fig. 3. Resistive transition of a three-dimensional network of  $10 \times 10 \times 10$  grains. The parameters used in this simulation are  $R_o = 0.32\Omega$  and  $I_{co} = 1.7mA$ . Each step should correspond to the creation of a layer of grains either in the normal or in the intermediate state through the network cross-section. Two different stages of the superconductor-normal transition in a 2-dimensional  $MgB_2$ -like network with  $10 \times 10$  grains. Orange dots represent the superconductive grains, dark blue dots represent the intermediate grains, green dots represent grains in the normal state. In (a), the first resistive layer (a strip in 2D) is formed. In (b), at slightly higher temperature the appearance of the second layer is shown. The parameters used in the simulation are :  $T_c = 39K$ ;  $R_o = 0.32\Omega$ ;  $I_b = 1mA$ ;  $I_{co} = 1.7mA$ .

separated and have a thickness of approximately one grain. Correspondingly, the resistance steps shown in Fig. 3 obey, as a good approximation, to a scaling law ( $R/R_o = 1/10$  in the present case). At the transition end, there is an intricacy of different layers and the resistance increases smoothly with the temperature.

The plots shown in Fig. 4 correspond to granular superconductors characterized by weak-links (YBCO-like). The simulation refers to the resistive transition of the weak-links. The grains, represented by the nodes of the network, remain in the superconductive state. Also in this case the transition occurs through the formation of resistive layers corresponding to resistance steps in the  $R$  vs  $T$  curve. Now what the algorithm can predict when temperature is lowered and the superconductive final state is achieved starting from the normal one is investigated. For this purpose, it is necessary to distinguish the  $I - V$  characteristics of resistively shunted underdamped, overdamped and generalized Josephson junctions [36]–[40]. We have routinely solved the Kirchhoff equations of the strong and weak links networks by using the underdamped, overdamped and generalized  $I - V$  characteristics and implementing a heating-cooling cycle around the critical temperature  $T_c$ . For all the three cases: (i) the conductance is  $G = 10^{10} S$  at  $I < I_c^i(T)$ , (ii) the normal state conductance  $G_o = 1/R_o$  at  $I > I_c^i(T)$  has been varied in the range  $1.0 - 10$  mA, (iii)  $G$  and  $G_o$  are much greater than the quantum conductance (i.e.  $g \gg 1$  always).

For the underdamped  $I - V$  characteristics, the intermediate states are characterized by voltage drop in the range  $0 < V < V_c^i(T)$  and current equal to  $I = I_c^i(T)$ . The intermediate states correspond to the coexistence of superconducting and normal domains. Upon current (voltage) decrease starting from the normal state, the behavior is always normal resistive, implying that the system reaches the superconductive ground state without exploring intermediate states.

For the overdamped  $I - V$  characteristics, the intermediate states are characterized by voltage drop in the range  $0 < V < 2V_c^i(T)$  and current in the range  $I_c^i(T) < I < I_c^i(2V_c^i(T))$ , as described by the function  $V = IR\sqrt{1 - (I_c/I)^2}$ , instead of a constant value. The behavior of the overdamped Josephson junction is the same upon increasing and decreasing the current (voltage).

For the general case, the  $I - V$  curve is partly hysteretic. Upon heating, the intermediate states are characterized by a voltage drop in the range  $0 < V < 2V_c^i(T)$  and current equal to  $I_c^i(T)$ . Conversely, upon cooling the intermediate states are described by the same equation of the overdamped case.

#### IV. DISCUSSION AND CONCLUSIONS

Several interesting aspects of the transition process in granular superconductors with weak and strong links emerge in these simulation. The main result is that the transition is not a continuous dynamical process, so that it can explain the large noise observed during the resistive transition of

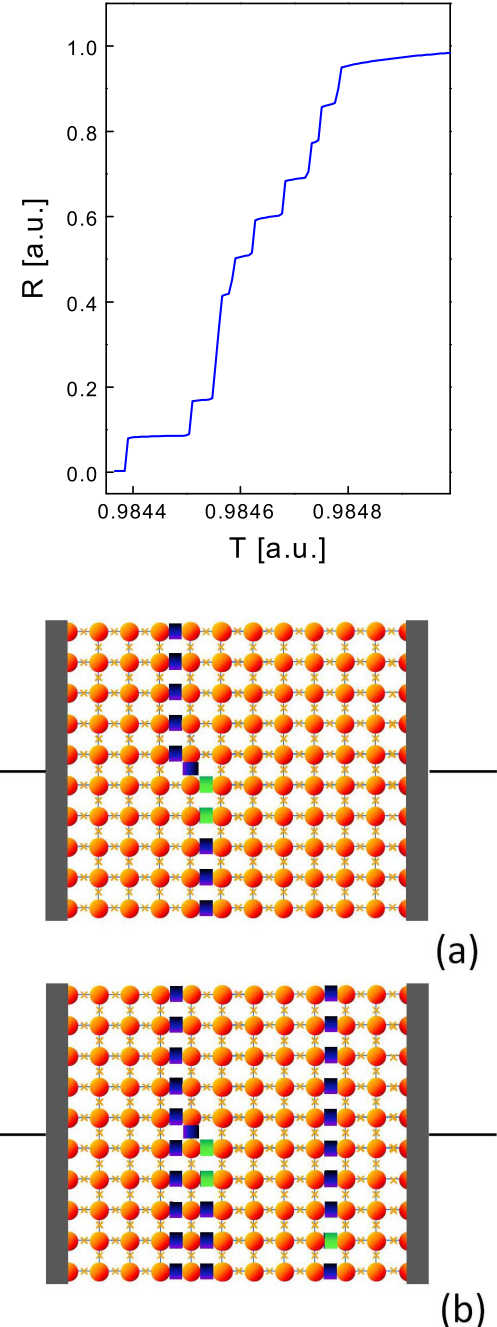


Fig. 4. Resistive transition of a three-dimensional network of  $10 \times 10 \times 10$  for weak-links with the parameters:  $R_o = 0.32\Omega$  and  $I_{co} = 1.7mA$ . Two different stages of the superconductor-normal transition in a 2-dimensional YBCO-like network with  $10 \times 10$  grains. Orange crosses represent weak-links in the superconducting state, green square represent resistive weak-links, while dark blue square represent weak-links in the intermediate state (We change symbol to let more evident the change). (a) shows the formation of the first resistive layer (a strip in 2D). (b) shows the transition at a temperature immediately following the appearance of the first layer. The parameters used in the calculations are:  $T_c = 65K$ ;  $R_o = 0.32\Omega$ ;  $I_b = 1mA$ ;  $I_{co} = 2.1mA$ .

polycrystalline high-temperature superconductors. A resistive layer is formed by the transition of a large number of grains simultaneously, approximately with the thickness of a single grain and orthogonal to the bias current density. This permits to evaluate the amplitude of the resistance steps generated by the layer formation in real specimens on the basis of the average grain size and specimen dimensions. Moreover, the relation between the layer formation and the transition noise at low-frequencies can be deduced by a scaling law, from the Campbell theorem. The present approach yields numerical solutions for the transition and a relation for the noise observed during the transition. By representing the superconducting film as a network of nonlinear resistors, it is possible to evaluate how the noisiness decreases at the end of the resistive transition, according to the variance of the distribution of the grain or of the weak-links critical currents. This is a crucial issue for the development of superconductor based sensors [41]–[43]. The steepness of the  $R$  vs  $T$  curve gives higher photon detection signals (photoresponse) at the expenses of an increase of the noise. Moreover, the resistance steps, corresponding to each layer formation, are visibly more squared and sharp for weak links than for strong-links transition. This fact may be related to the different slopes of the relative voltage noise spectra reported in Refs. [19], [21].

#### ACKNOWLEDGMENT

The Istituto Superiore Boella is gratefully acknowledged for financial support.

#### REFERENCES

- [1] C. Heiden and G. I. Rochlin, Phys. Rev. Lett. **21**, 691 (1968).
- [2] S. Field, J. Witt, F. Nori and X. Ling, Phys. Rev. Lett. **74**, 1206 (1995).
- [3] A.C. Marley, M.J. Higgins, S. Bhattacharya, Phys. Rev. Lett. **74**, 3029 (1995).
- [4] S.H. Chun, W. Song, G.H. Koh, H.C. Kim, Z.G. Khim, Physica C **282**, 2335 (1997).
- [5] Y. Togawa, R. Abiru, K. Iwaya, H. Kitano, A. Maeda, Phys. Rev. Lett. **85**, 3716 (2000).
- [6] C. Reichhardt, C.J. Olson, J. Groth, S.B. Field and F. Nori, Phys. Rev. B **53**, R8898 (1996).
- [7] Q.M. Lu, C.J.O. Reichhardt, C. Reichhardt, Phys. Rev. B **75**, 054502 (2007).
- [8] C. De Leo, IEEE Trans. Appl. Supercond. **18**, 1769 (2008).
- [9] R. Kato and Y. Enomoto, Physica C **426**, 110 (2005).
- [10] J. Das, T.J. Bullard and V.C. Tuber, Physica A **318**, 48 (2003).
- [11] L.D. Landau, Phys. Z. Sov. Union **11**, 129 (1937).
- [12] G.L. Ginzburg and L.D. Landau, Phys. Abh. Sov. Union **1**, 7 (1958).
- [13] M.A. Lindeman et al. Nucl. Instr. & Methods A, **599**, 715 (2006).
- [14] G.W. Fraser, Nucl. Instr. & Methods A **523**, 234 (2004).
- [15] D. Brandt, G.W. Fraser, D.J. Raine, C. Binns, J. Low Temp. Phys. **151**, 25 (2008).
- [16] A. Carbone, B.K. Kotowska, D. Kotowski, Phys. Rev. Lett. **95**, 236601 (2005).
- [17] S. Jobaud, A. Petrosyan, S. Ciliberto, and N.B. Garnier, Phys. Rev. Lett. **100**, 180601 (2008).
- [18] A. Bid, A. Guha, A.K. Raychaudhuri, Phys. Rev. B **67**, 174415 (2003).
- [19] P. Mazzetti, C. Gandini, A. Masoero, M. Rajteri and C. Portesi, Phys. Rev. B **77**, 64516 (2008).
- [20] L. Ponta, A. Carbone, M. Gilli, P. Mazzetti, Phys. Rev. B **79**, 134513 (2009).
- [21] P. Mazzetti, A. Stepanescu, P. Tura, A. Masoero and I. Puica, Phys. Rev. B **65**, 132512 (2002).
- [22] I.S. Beloborodov, A.V. Lopatin, V.M. Vinokur, K.B. Efetov, Rev. Mod. Phys. **79**, 469 (2007).
- [23] K.B. Efetov, Sov. Phys. JETP **51**, 1015 (1980).
- [24] H.M. Jaeger, D.B. Haviland, A.M. Goldman and B.G. Orr, Phys. Rev. B **34**, 4920 (1986); B.G. Orr, H.M. Jaeger, A.M. Goldman and C.G. Kuper, Phys. Rev. Lett. **56**, 378 (1986).
- [25] S. Chakravarty, G.L. Ingold, S. Kivelson, G. Zimany, Phys. Rev. B **37**, 3283 (1988); S. Chakravarty, G.L. Ingold, S. Kivelson, A. Luther, Phys. Rev. Lett. **56**, 2303 (1986).
- [26] H. Hilgenkamp, J. Manhart, Rev. Mod. Phys. **74**, 485 (2002).
- [27] D.C. Larbalestier et al. Nature **410**, 186 (2001).
- [28] X.X. Xi, Rep. Prog. Phys. **71**, 116501 (2008).
- [29] H. Shimakage, Z. Wang, IEEE Trans. Appl. Supercond. **17**, 202 (2007).
- [30] Y.W. Kim, S.G. Lee, IEEE Trans. Appl. Supercond. **17**, 206 (2007).
- [31] S. Li, T. White, J. Plevert and C.Q. Sun, Supercond. Sci. Technol. **17**, S589 (2004).
- [32] O.F. de Lima and C.A. Cardoso, Physica C **386**, 575 (2003).
- [33] S. Sen, A. Singh, D.K. Aswal, S.K. Gupta, J.V. Yakhmi, V.C. Sahni, E.M. Choi, H.J. Kim, K.H.P. Kim, H.S. Lee, W.N. Kang and S.I. Lee, Phys. Rev. B **65**, 214521 (2002).
- [34] E.M. Choi, H.J. Kim, S. K. Gupta, P. Chowdhury, K.H.P. Kim, S.I. Lee, W.N. Kang, H.-Jin K., M.H. Jung and S.H. Park, Phys. Rev. B **69**, 224510 (2004).
- [35] W.D. Markiewicz and J. Toth, Cryogenics **46**, 468 (2006).
- [36] T.P. Orlando and K.A. Delin, *Foundation of Applied Superconductivity*, Prentice Hall (1991).
- [37] P.D. Dresselhaus, S.P. Benz, C.J. Burroughs, et al. IEEE Trans. Appl. Supercond. **17**, 173 (2007).
- [38] W. Yu, D. Stroud, Phys. Rev. B **46**, 21 (1992).
- [39] R. Fazio, H. van der Zant, Phys. Rep. **355**, 235 (2001).
- [40] A.H. Majedi, IEEE Trans. Appl. Supercond. **17**, 617 (2007).
- [41] G. N. Gol'tsman, O. Okuney, G. Chulkova, A. Lipatov, A. Semenov, K. Smirnov, B. Voronov, A. Dzardanov, C. Williams and R. Sobolewski, Appl. Phys. Lett. **79**, 705 (2001).
- [42] A.J. Kreisler, A. Gaugue, Supercond. Sci. Tech. **13**, 1235 (2000).
- [43] F. Rahman, Contemporary Physics **47**, 181 (2006).
- [44] The MATLAB code used in this work can be downloaded at [www.polito.it/noiselab/utilities](http://www.polito.it/noiselab/utilities)